



OPEN ACCESS

EDITED BY

Nenad Filipović,
Faculty of Agriculture, University of
Belgrade, Serbia

REVIEWED BY

Ozlem Sen,
Italian Institute of Technology (IIT), Italy
John Gallagher,
Dublin City University, Ireland
Zanka Bojic-Trbojevic,
Institute for the Application of Nuclear
Energy (INEP), Serbia

*CORRESPONDENCE

Yulan Gu,
guyulan@263.net
Chuandan Wan,
cd_wan@163.com
Dengfeng Zou,
zdf1226@126.com

SPECIALTY SECTION

This article was submitted to Medicinal
and Pharmaceutical Chemistry,
a section of the journal
Frontiers in Chemistry

RECEIVED 11 April 2022

ACCEPTED 26 July 2022

PUBLISHED 29 August 2022

CITATION

Shi X, Gu Y, Wan C, Jiang X, Shen L,
Tan L, Zhong Y and Zou D (2022), Two
copper(II) compounds derived from
tetrazole carboxylates for
chemodynamic therapy against
hepatocellular carcinoma cells.
Front. Chem. 10:915247.
doi: 10.3389/fchem.2022.915247

COPYRIGHT

© 2022 Shi, Gu, Wan, Jiang, Shen, Tan,
Zhong and Zou. This is an open-access
article distributed under the terms of the
[Creative Commons Attribution License
\(CC BY\)](https://creativecommons.org/licenses/by/4.0/). The use, distribution or
reproduction in other forums is
permitted, provided the original
author(s) and the copyright owner(s) are
credited and that the original
publication in this journal is cited, in
accordance with accepted academic
practice. No use, distribution or
reproduction is permitted which does
not comply with these terms.

Two copper(II) compounds derived from tetrazole carboxylates for chemodynamic therapy against hepatocellular carcinoma cells

Xinya Shi¹, Yulan Gu^{1*}, Chuandan Wan^{2*}, Xin Jiang³, Lei Shen⁴,
Litao Tan⁴, Yujie Zhong⁴ and Dengfeng Zou^{3*}

¹Changshu No. 2 People's Hospital, Changshu, Jiangsu, China, ²Central Laboratory of Changshu
Medical Examination Institute, Changshu, China, ³School of Pharmacy, Guilin Medical University,
Guilin, China, ⁴Department of Materials Engineering, Changshu Institute of Technology, Changshu,
China

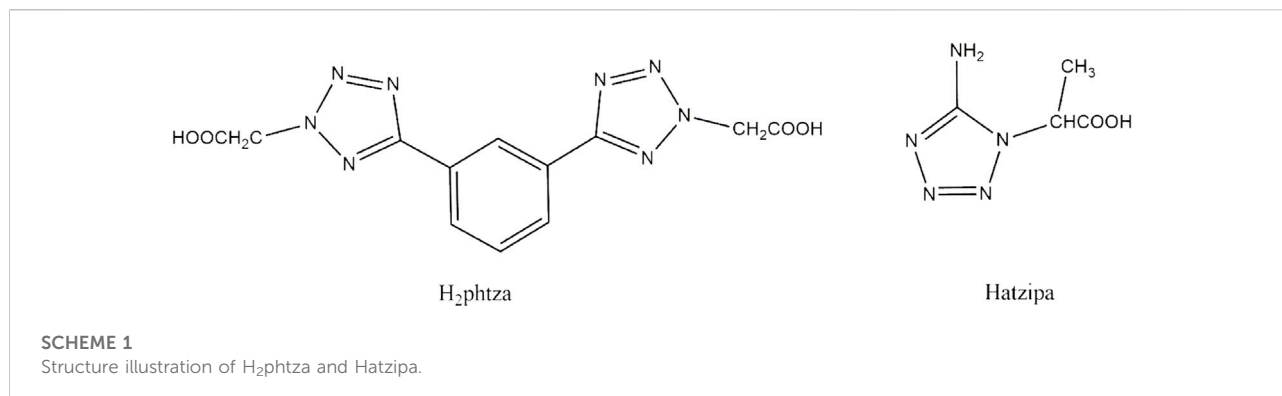
Two Cu(II) compounds based on tetrazole-carboxylate ligands, [Cu(phtza)₂(H₂O)₂]-3H₂O (**1**) and [Cu(atzipa)₂]-2H₂O (**2**) (phtza = 2,2'-(5,5'-(1,3-phenylene)bis(2*H*-tetrazole-5,2-diyl))diacetate, atzipa = 3-(5-amino-1*H*-tetrazol-1-yl)isopropanoic anion), were designed and synthesized by hydrothermal reactions. The X-ray diffraction results show that the two compounds show two-dimensional (2D) layer structures. Nanoprecipitation with 1,2-distearoyl-sn-glycero-3-phosphoethanolamine-N-[methoxy(polyethylene glycol)-2000] (DSPE-PEG-2000) contributes to the formation of the nanoparticles (NPs) with excellent water dispersity. *In vitro* study indicates that the two NPs exert considerable cytotoxicity toward human hepatocellular carcinoma cells (HepG2 and Huh7) with low half-maximal inhibitory concentration (IC₅₀). However, the cytotoxicity of such NPs is negligible in normal cells (HL-7702). The cytotoxicity of these NPs was also investigated by the flow cytometry and Calcein-AM/PI (live/dead) co-stained experiments. The results promise the great potential of these NPs for chemodynamic therapy against cancer cells.

KEYWORDS

Cu(II), tetrazole carboxylate, human hepatocellular carcinoma cells, chemodynamic therapy, *in vitro*

Introduction

Cancer has already become a tremendous threat to health worldwide, following heart and cardiovascular diseases, and global mortality keeps rising (Siegel et al., 2018). Traditional therapeutic methods, for example, chemotherapy usually employs drugs, such as cisplatin (II) and doxorubicin, for the treatment of cancer (Tang et al., 2018; Song et al., 2019; Zhu et al., 2020). Normal cells may still suffer from side effects because the targeting ability of the compounds is very poor, though such drugs achieve considerable



therapeutic efficacy to some extent. Therefore, designing and synthesizing anticancer drugs with specific targeting ability to avoid the side effects and enhance the therapeutic efficacy is an effective alternative to solve the problem (Fujita et al., 2014; Weiss et al., 2014; Sun et al., 2017a; Sun et al., 2017b; Yang et al., 2018; Yang et al., 2019a; Yang et al., 2019b; Yang et al., 2020; Zou et al., 2020). Tumor microenvironment (TME), usually features hypoxia and high hydrogen peroxide (H₂O₂) concentration, compared with that in normal tissues (Arneth, 2020; Deng et al., 2020). Chemodynamic therapy (denoted as CDT) can induce cell death by catalyzing H₂O₂ to generate cytotoxic hydroxyl radicals (\cdot OH) through Fenton or Fenton-like reactions, typically Fe(II) or Cu(II) compounds (Fujita et al., 2014; Li et al., 2018; Yang et al., 2019c; Shen et al., 2019; Li et al., 2020). For example, Chen *et al.* designed a kind of nanosystem that is able to generate free radicals by iron pool for cancer chemodynamic therapy (H Zou et al., 2021). CDT is considered a non-invasive strategy to fight against cancer.

Coordination compounds, a class of functional materials, are attracting increasing interest owing to not only their diverse structures but also their great potential in the field of luminescence, adsorption, and catalysis (Aromi et al., 2011; Wriedt et al., 2012; Zou et al., 2014a; Zou et al., 2015a; Du et al., 2015; Shen et al., 2016; Zhang et al., 2016; Lin et al., 2019; Zou et al., 2021). Tetrazole carboxylates are bi-functional ligands with either flexible carboxylate groups or rigid tetrazole rings that have great potential for constructing a variety of coordination architectures. These ligands with abundant nitrogen and oxygen atoms have a high possibility to show diverse coordination modes, and the CH₂ is capable of favoring the carboxylate with flexible orientations, contributing to the formation of novel crystal structures (Zou et al., 2014b; Zou et al., 2014c; Zou et al., 2014d; Zou et al., 2015b; Dai et al., 2021). In the previous study, tetrazole-based ligands have been universally employed as multi-building blocks for the construction of novel coordination architectures and in the fields of luminescence (Zou et al., 2014b; Zou et al., 2014c; Zou et al., 2014d; Yang et al., 2014; Zou et al., 2015b; Sun et al., 2016;

Zhang et al., 2016; Dai et al., 2021), catalysis (Zou et al., 2015a), and adsorption (Wriedt et al., 2012). However, the biological applications of such compounds are relatively less reported. Based on the observations, we are devoted to designing and synthesizing novel Cu(II) compounds based on two different tetrazole carboxylates, 2,2'-(5,5'-(1,3-phenylene)bis(2H-tetrazole-5,2-diyl))diacetic acid (Hphtza) and Hatzipa = 3-(5-amino-1H-tetrazol-1-yl)isopropanoic acid (Scheme 1). As a result, [Cu(phtza)₂(H₂O)₂] \cdot 3H₂O (**1**) and [Cu(atzipa)₂] \cdot 2H₂O (**2**) were obtained by hydrothermal reactions. The nanoparticles (NPs) of the two compounds were synthesized by a nano-precipitation method with encapsulation by 1,2-distearoyl-sn-glycero-3-phosphoethanolamine-N-[methoxy(polyethylene glycol)-2000] (DSPE-PEG-2000). Further *in vitro* study suggests the two NPs show high cytotoxicity toward human hepatocellular carcinoma cells (HepG2 and Huh7). In terms of cytotoxicity, compound **1** is superior to compound **2** on HepG2 (IC₅₀: 58.3 μ M for compound **1** NPs and 83.6 μ M for compound **2** NPs), while both complexes have IC₅₀ values of 45.5 μ M on Huh7 cells. Eventually, the Calcein-AM/PI (PI = 3,8-diamino-5-(3-diethylaminopropyl)-6-phenylphenanthridinium iodide) staining and flow cytometry results demonstrate that these compounds are able to induce cell apoptosis for efficient chemodynamic therapy.

Experimental section

Materials and apparatus

H₂phtza and Hatzipa were prepared according to the literature (Yang et al., 2014; Sun et al., 2016). The chemicals were commercially available from Sigma-Aldrich (Shanghai). Elemental analyses (C, H, and N) were performed with a PE2400 elemental analyzer. The Fourier transform infrared (FT-IR) spectrum was measured on the Thermo NICOLET 380 instrument as a KBr disk (4,000–400 cm⁻¹). The UV-vis

TABLE 1 Selected crystal data of compounds **1** and **2**.

Compound	1	2
Empirical formula	C ₁₂ H ₁₈ CuN ₈ O ₉	C ₈ H ₁₆ CuN ₁₀ O ₆
Formula mass	481.88	411.85
Crystal system	Monoclinic	Monoclinic
Space group	<i>P2₁/c</i>	<i>P2₁/c</i>
<i>a</i> (Å)	16.736 (3)	5.1139 (14)
<i>b</i> (Å)	13.127 (2)	12.271 (3)
<i>c</i> (Å)	8.5308 (13)	12.598 (3)
α (°)	90.00	90
β (°)	90.407 (4)	106.139 (9)
γ (°)	90.00	90
<i>V</i> (Å ³)	1874.1 (5)	759.4 (3)
<i>Z</i>	4	2
<i>T</i> (K)	291	293 (2)
D _{calcd} (g·cm ⁻³)	2.074	1.668
μ (mm ⁻¹)	1.23	1.49
Reflections collected	12,577	3,934
Unique reflections (<i>R</i> _{int})	4,291 (0.0604)	1,333 (0.041)
<i>R</i> ^[a] and <i>wR</i> ^[b]	0.0525 and 0.1404	0.041 and 0.1261
GOF ^[c]	0.974	1.015
$\Delta\rho_{\max}$ (e/Å ³)	0.70	0.54
$\Delta\rho_{\min}$ (e/Å ³)	-1.134	-0.41

^a*R* = $\sum |F_o| - |F_c| / \sum |F_o|$.

^b*R*_w = $\{ \sum w(F_o^2 - F_c^2)^2 / \sum w(F_o^2)^2 \}^{1/2}$.

^cGOF = $\{ \sum w(F_o^2 - F_c^2)^2 / (n-p) \}^{1/2}$, where *n* = number of reflections and *p* = total number of parameters refined.

spectra were obtained from a UV-3600 spectrometer (Shimadzu, Japan).

Preparation and characterization of compounds **1** and **2**

A mixture of Cu(NO₃)₂·3H₂O (241 mg, 0.1 mmol) and H₂phtza (165 mg, 0.05 mmol) in a mixture of water (2 ml) and ethanol (2 ml) was sealed in a stainless steel container and heated at 120°C for 24 h. After cooling to room temperature, the solution was filtered for evaporation. Blue crystals were obtained. Elemental analyses Calcd. for C₁₂H₁₈CuN₈O₉ (%): C, 29.91; H, 3.74; N, 23.25. Found (%): C, 29.73; H, 3.77; N, 23.40. IR (KBr, cm⁻¹): 3,022 (w), 2,901 (w), 2,245(w), 1,623 (m), 1,577 (m), 1,521 (s), 1,124 (vs), 1,088 (s), 935 (w), 868 (m), 725 (m), and 623 (s).

The synthesis procedure for compound **2** is similar to that of **1** except that H₂phtza has been replaced by Hatzipa (79 mg, 0.05 mmol). Elemental analyses Calcd. for C₃₆H₃₂Cl₂CuN₈O₁₀ (%): C, 23.33; H, 3.88; N, 34.00. Found (%): C, 23.43; H, 3.82; N, 34.50. IR (KBr, cm⁻¹): 3,440 (m), 3,088 (w), 2,933 (w), 1,635 (w),

TABLE 2 Selected bond distances (Å) and angles (°) for compounds **1** and **2**.

Compound **1**

Cu(1)–O(1)	1.936 (3)	Cu(1)–O(3A)	1.977 (3)
Cu(1)–O(6)	1.957 (3)	Cu(1)–O(4B)	2.210 (3)
Cu(1)–O(5)	1.973 (3)	O(1)–Cu(1)–O(6)	90.75 (14)
O(1)–Cu(1)–O(5)	90.87 (14)	O(6)–Cu(1)–O(5)	175.83 (16)
O(1)–Cu(1)–O(3A)	174.93 (13)	O(6)–Cu(1)–O(3A)	87.39 (14)
O(5)–Cu(1)–O(3A)	90.68 (14)	O(1)–Cu(1)–O(4B)	92.62 (12)
O(6)–Cu(1)–O(4B)	96.22 (15)	O(5)–Cu(1)–O(4B)	87.54 (14)
O(3A)–Cu(1)–O(4B)	92.27 (12)		

Compound **2**

Cu(1)–O(1)	1.943 (3)	N(4)–Cu(1D)	1.999 (3)
Cu(1)–O(1A)	1.943 (3)	N(4B)–Cu(1)–N(4C)	180.0
Cu(1)–N(4B)	1.999 (3)	C(1)–O(1)–Cu(1)	120.6 (3)
Cu(1)–N(4C)	1.999 (3)	C(4)–N(4)–Cu(1D)	132.6 (3)
O(1)–Cu(1)–O(1A)	180.0 (2)	N(4)–N(4)–Cu(1D)	120.8 (3)
O(1)–Cu(1)–N(4B)	87.56 (13)	O(1A)–Cu(1)–N(4B)	92.44 (13)
O(1)–Cu(1)–N(4C)	92.44 (13)	O(1A)–Cu(1)–N(4C)	87.56 (13)
Cu(1D)–N(4)–C(4)–N(1)	177.0 (3)		

Symmetry code: For **1**: A: *x*+1, *-y*+3/2, *z*+1/2; B: *x*+1, *y*, *z*+1; C: *x*-1, *-y*+3/2, *z*-1/2. For **2**: A: *-x*+1, *-y*, *-z*+1; B: *x*, *-y*+1/2, *z*+1/2; C: *-x*+1, *y*-1/2, *-z*+1/2; D: *-x*+1, *y*+1/2, *-z*+1/2.

1,568 (m), 1,494 (s), 1,385 (m), 1,114 (vs), 925 (w), 855 (w), 738 (m), and 629 (s).

Crystal structure determination

Suitable single crystals of **1** and **2** were selected for collection of intensity data on a Bruker SMART APEX II CCD diffractometer using a ϕ - ω scan mode at 291 K for compound **1** and 296(2) K for compound **2** [monochromate Mo *K*_α radiation (λ = 0.71073 Å)]. SADABS was applied for multi-scan absorption corrections of all intensity data. The structures were solved by direct methods, and SHELXTL software was used to refine *F*² by full-matrix least squares procedures (Sheldrick, 2008). All hydrogen atoms were fixed in calculated positions and refined isotropically. The crystallographic data of compounds **1** and **2** are listed in Table 1. The selected bond lengths and angles are shown in Table 2. The hydrogen bond parameters are listed in Supplementary Table S1.

Hydroxyl generation by Fenton-like reaction

10 μ g mL⁻¹ MB, 8 mM H₂O₂, and 0.5 mM compounds **1** or **2** NPs were allowed to stand at 37°C for 30 min. The OH-induced

MB degradation was monitored by the absorbance change at 665 nm.

Synthesis of compounds 1 and 2 nanoparticles

The nanoparticles (NPs) were prepared by nanoprecipitation with DSPE-PEG₂₀₀₀. A mixture of DSPE-PEG₂₀₀₀ (10 mg) and compound **1** or **2** (2 mg) was dissolved in tetrahydrofuran (THF) under ultrasound (100 W). Then, such a solution was injected into 5 ml distilled water under ultrasound. After the mixture was sonicated in an ultrasonic washer for 3–5 days, THF was removed by purging nitrogen gas at room temperature. The solution was stored at 4°C for characterization and cytotoxicity experiment.

Cell culture and cytotoxicity assay

Hepatocellular carcinoma cell lines (HCC, including HepG2 and Huh7) and human normal cells (HL-7702) were available from the Shanghai Institute of Biochemistry and Cell Biology, Chinese Academy of Sciences (CAS). HepG2 and Huh7 cells were cultured in DMEM (Biosharp; Biosharp Life Sciences) with 10% FBS (Biosharp; Biosharp Life Sciences) at 37°C with 5% CO₂.

Cell viability was determined using a Cell Counting Kit. HepG2 cells (2×10^3 /well), Huh7 cells (2×10^3 /well), and HL-7702 (2×10^3 /well) were seeded into 96-well plates. The cells were cultured with the NPs of compounds **1** and **2** for 24 h, respectively. Cytotoxicity was evaluated using the Cell Counting Kit-8 (CCK-8, Abbkine Scientific). CCK-8 was added to the medium and incubated with the cells for 2 h. Then, the absorbance was measured on a microplate reader. The cell viability was calculated as follows:

$$\text{Relative cell viability (\%)} = (A_{\text{treatment}} / A_{\text{control}}) \times 100\%$$

where $A_{\text{treatment}}$ = mean absorbance of the medium from cells incubated with NPs containing complex **1** or **2** and A_{control} = mean absorbance of the medium incubated without NPs of non-treated cells. The half-maximal inhibitory concentration (IC₅₀) was calculated using SPSS 25.0 software.

The MTT assay was repeated three times.

Flow cytometry

Cell apoptosis of the nanoparticles was detected by flow cytometry. Generally, HepG2 cells (2×10^5 /well) and Huh7 cells (2×10^5 /well) were seeded in 6-well plates and cultured for 24 h. Then, the cells were co-cultured with NPs of compound **1** or **2** for 24 h at the concentration of IC₅₀ and $2 \times$ IC₅₀, respectively. Cell apoptosis was detected by the FITC Annexin V Apoptosis

Detection Kit I on the flow cytometry (Attune NxT, Invitrogen by Thermo Fisher Scientific). The flow cytometry was repeated three times.

Live/dead co-staining by Calcein-AM and PI

HepG2 and Huh7 (both concentration $\sim 2 \times 10^4$ /well) were seeded in 24-well plates. In this experiment, we set up control groups, IC₅₀ groups and $2 \times$ IC₅₀ groups, respectively. Calcein AM is a cell-permeant dye that can be used to determine cell viability in most eukaryotic cells. In live cells, the non-fluorescent calcein AM is converted to a green-fluorescent calcein after acetoxymethyl ester hydrolysis by intracellular esterases. Calcein AM is used to stain live cells (green channel), while PI is used to stain dead cells (red channel). In the control group, the cells were cultured, and then the cells were treated with compounds **1** and **2** NPs for 24 h at the concentration of IC₅₀ and $2 \times$ IC₅₀, respectively. Then, the medium was discarded, and the cells were washed with PBS three times. The cells were co-stained with a Living/Dead cell double staining kit (Sigma-Aldrich (Shanghai) Trading Co., Ltd.) with the concentration of calcein-AM at 2.5 μM and PI 4.5 μM, respectively. After 20 min, the cells were washed with PBS three times. The photographs were captured on an inverted fluorescence microscope, Olympus FV1000 confocal microscope.

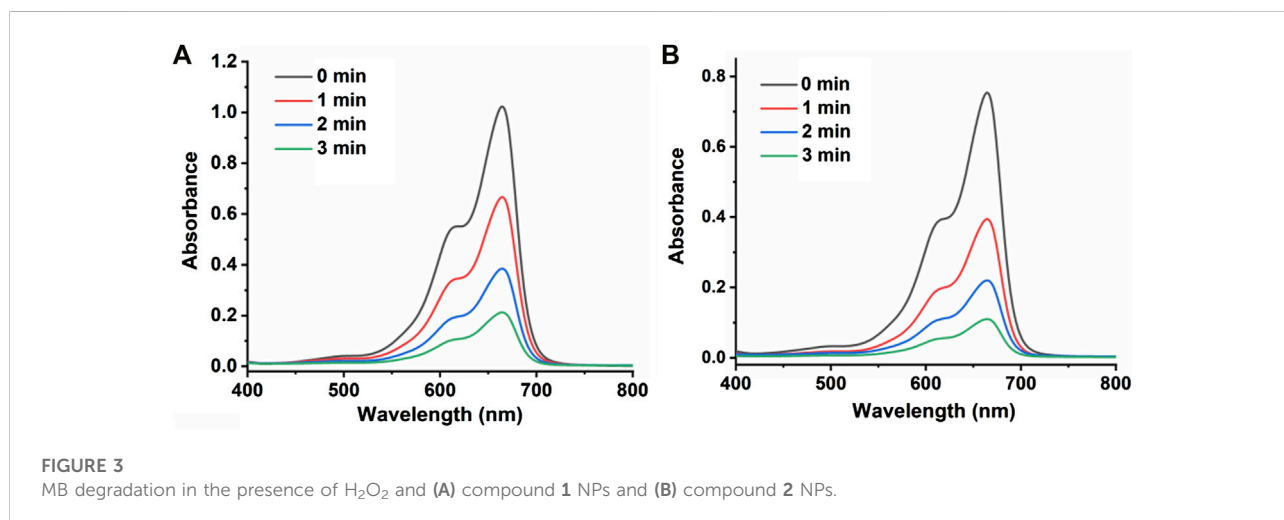
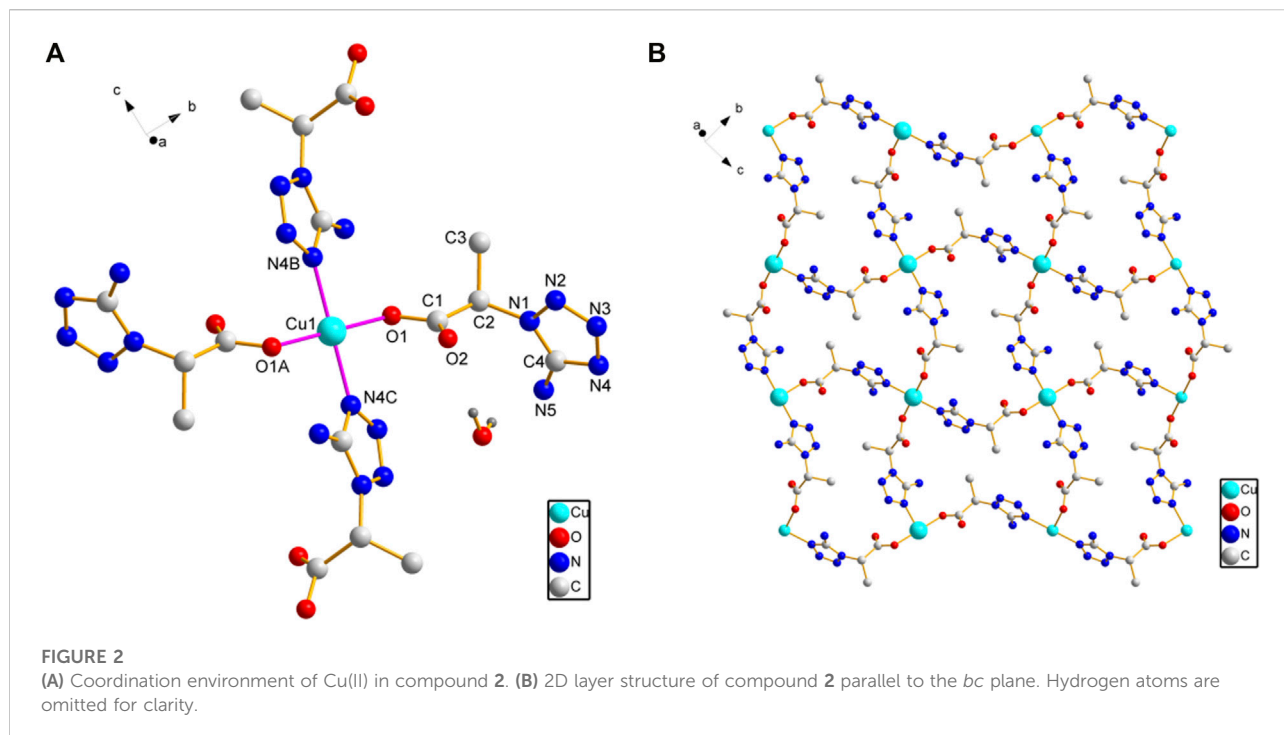
Statistical analysis

All numeric data are expressed as mean \pm s.d. unless otherwise indicated. The significance between the two groups was analyzed by a two-tailed Student's *t*-test. Statistical analysis was performed using GraphPad Prism 6.0. *p* values of less than 0.05 were considered significant (***p* < 0.01 and ****p* < 0.01).

Results and discussions

Description of crystal structures of [Cu(phtza)₂(H₂O)₂].3H₂O (**1**) and [Cu(atzipa)₂].2H₂O (**2**)

X-ray crystallography results reveal that both compounds **1** and **2** crystallize in monoclinic lattice with space group *P*₂₁/*c*. Compound **1** is made up of one Cu(II), two phtza[−] anions, two coordinated water, and three lattice water molecules, while compound **2** consists of one Cu(II), two atzipa[−] anions, and two lattice water (Figures 1A, 2A). The phtza ligand is a tetradentate to bridge the adjacent Cu(II) centers by two carboxylate oxygen atoms in a $\mu_{1,1,3}$ -COO or a μ_1 -COO mode, respectively, to generate a two-dimensional (2D) layer structure parallel to the *ac* plane (Figure 1B). In contrast, atzipa in compound **2**



hydrogen bonding to generate a three-dimensional (3D) supramolecular structure (Supplementary Figures S1, S2; Supplementary Table S1). Compared with the previously reported mononuclear $[\text{Cu}(\text{2-pytzipa})_2(\text{H}_2\text{O})_2] \cdot 2\text{H}_2\text{O}$ (Zhai et al., 2017) (2-pytzipa = 5-(2-pyridyl)tetrazole-2-isopropanoic anion) in which 2-pytzipa only adopts the N (pyridyl) and N(tetrazole) chelating mode, the coordination modes of phtza and atzipa are more complicated. 3-pytza in $[\text{Cu}(\text{3-pytza})_2(\text{H}_2\text{O})]_n \cdot 2n\text{H}_2\text{O}$ (Zou et al., 2014e) shows a N(pyridyl) and O (COO^-) bridging mode, which is similar to

that of atzipa in compound 2. All the nitrogen atoms in phtza in compound 1 are all uncoordinated.

Since methylene blue (MB) can be degraded by hydroxyl radicals, the hydroxyl radicals' generation ability of compounds 1 and 2 NPs was investigated by recording the absorbance of methylene blue (MB) in the presence of H_2O_2 (Figure 3). The absorbance of MB continued to decrease because of the generation of hydroxyl radicals catalyzed by the Fenton-like reaction of compounds 1 or 2 NPs and H_2O_2 . In addition, compound 1 NPs are superior to compound 2 NPs in terms of catalysis.

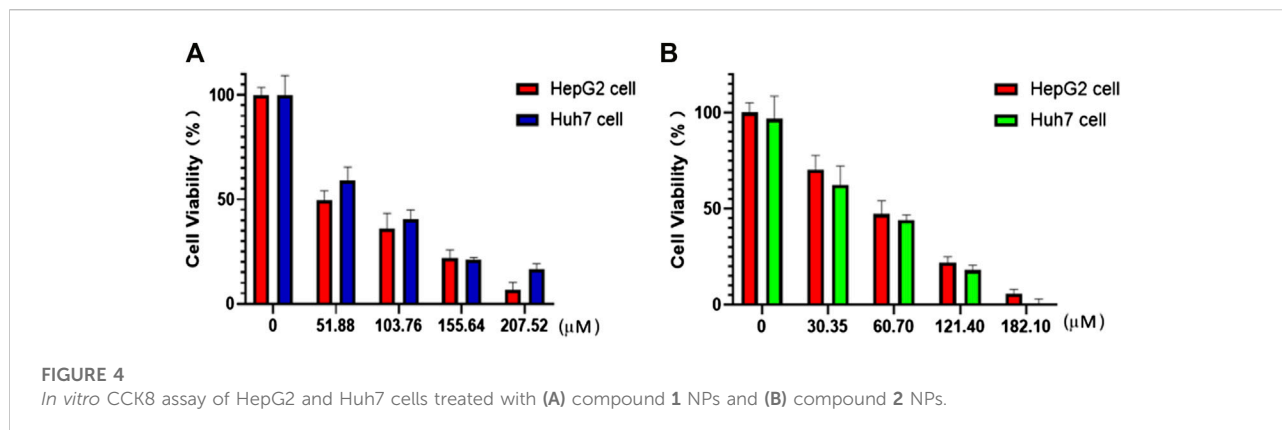


TABLE 3 Comparison of cytotoxicity of Cu(II) compounds based on tetrazole ligands.

Compound	Cell lines	IC ₅₀ (μM)	References
[Cu(atzpa) ₂]	HeLa	10.9	Zhang et al. (2021)
[Cu(pytzpa) ₂]	HeLa	6.7	Zhang et al. (2021)
[Cu(2-pytzpa) ₂ (H ₂ O) ₂].2H ₂ O	HeLa	70.0	Zhai et al. (2017)

atzpa = 3-(5-amino-tetrazol-1-yl)-propionic anion, pytzpa = 2-(5-pyridin-3-yl-tetrazol-2-yl)-propionic anion, and 2-pytzpa = 5-(2-pyridyl)tetrazole-2-isopropanoic anion.

TABLE 4 Apoptosis rate of compounds 1 and 2 NPs on HepG2 and Huh7 cells.

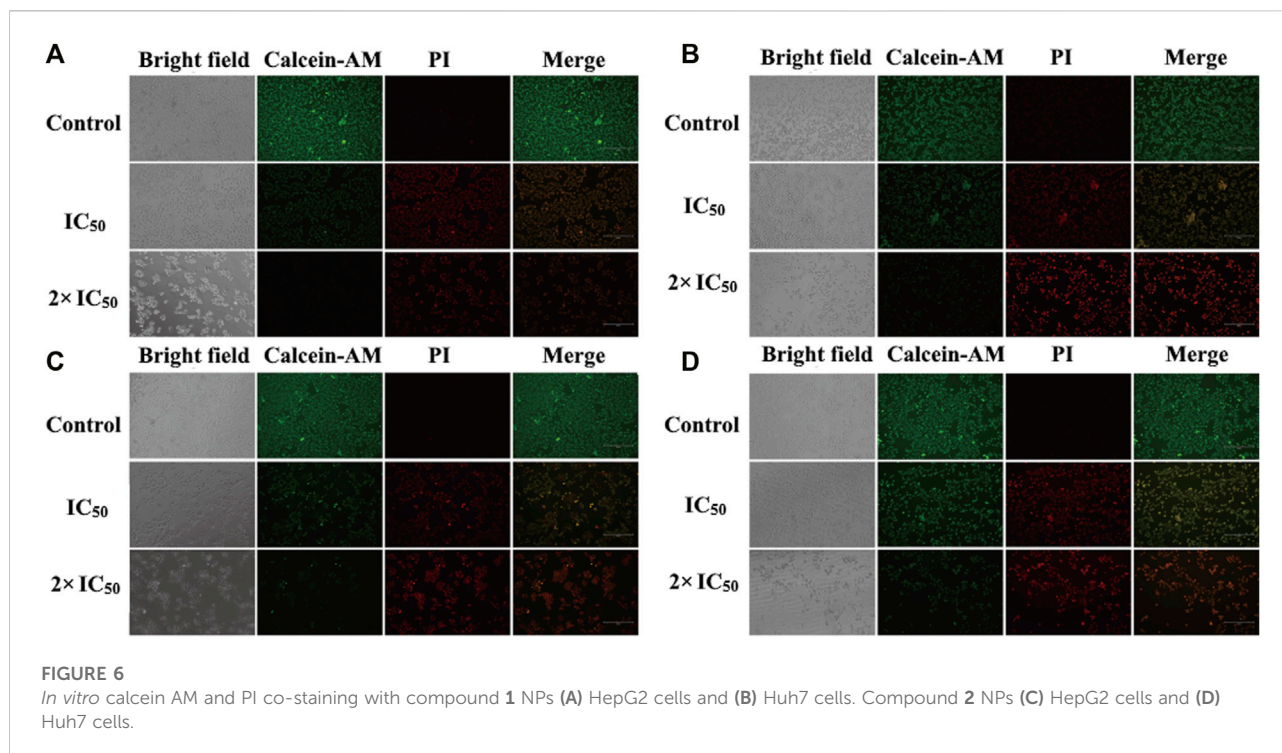
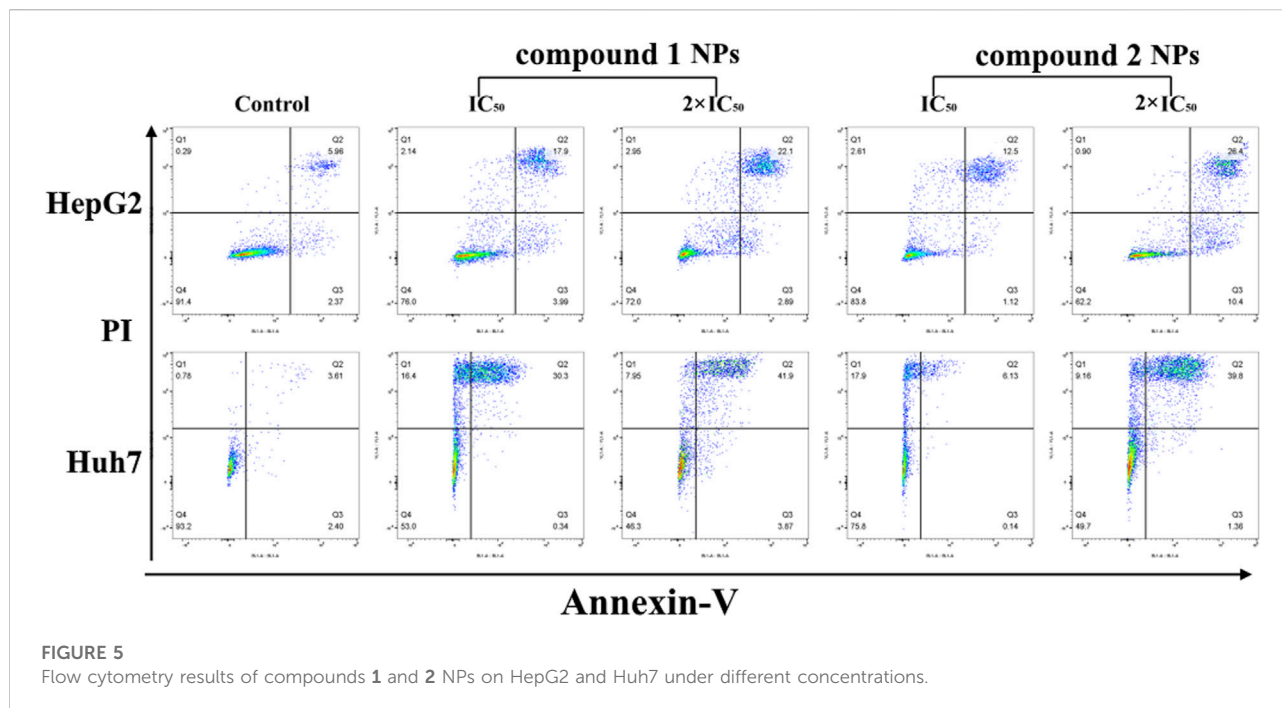
	Control (%)	Compound 1 NPs		Compound 2 NPs	
		IC ₅₀ (%)	2 × IC ₅₀ (%)	IC ₅₀ (%)	2 × IC ₅₀ (%)
HepG2	9.94 ± 2.79	17.27 ± 3.99	20.16 ± 4.87	15.46 ± 1.59	43.33 ± 5.66
Huh7	6.01 ± 0.00	25.09 ± 5.31	42.06 ± 3.61	15.79 ± 11.09	33.04 ± 8.19

Cytotoxicity and flow cytometry

The nanoparticles (NPs) of compounds 1 and 2 were prepared by nanoprecipitation with DSPE-PEG₂₀₀₀ due to their excellent dispersity and stability in aqueous solution. Two different human hepatocellular carcinoma cells, HepG2 and Huh7, were chosen to investigate the chemodynamic therapeutic efficacy of NPs of compounds 1 and 2 by the Cell Counting Kit-8 (CCK-8) assay. CCK-8 allows sensitive colorimetric assays for the determination of cell viability in cell proliferation and cytotoxicity assays. The results showed concentration-dependent cell death after two types of liver cancer cells were treated with NPs of compound 1 or 2 under different concentrations (Figure 4). With the increase of the concentrations, the viability of HepG2 and Huh7 cells tends to gradually reduce. For HepG2 cells, the IC₅₀ values of compounds 1 and 2 NPs are 58.3 and 83.6 μM, respectively. For Huh7 cells, the IC₅₀ of both NPs is 45.5 μM. Both compounds have strong inhibitory effects on the cell activity of the two cell lines.

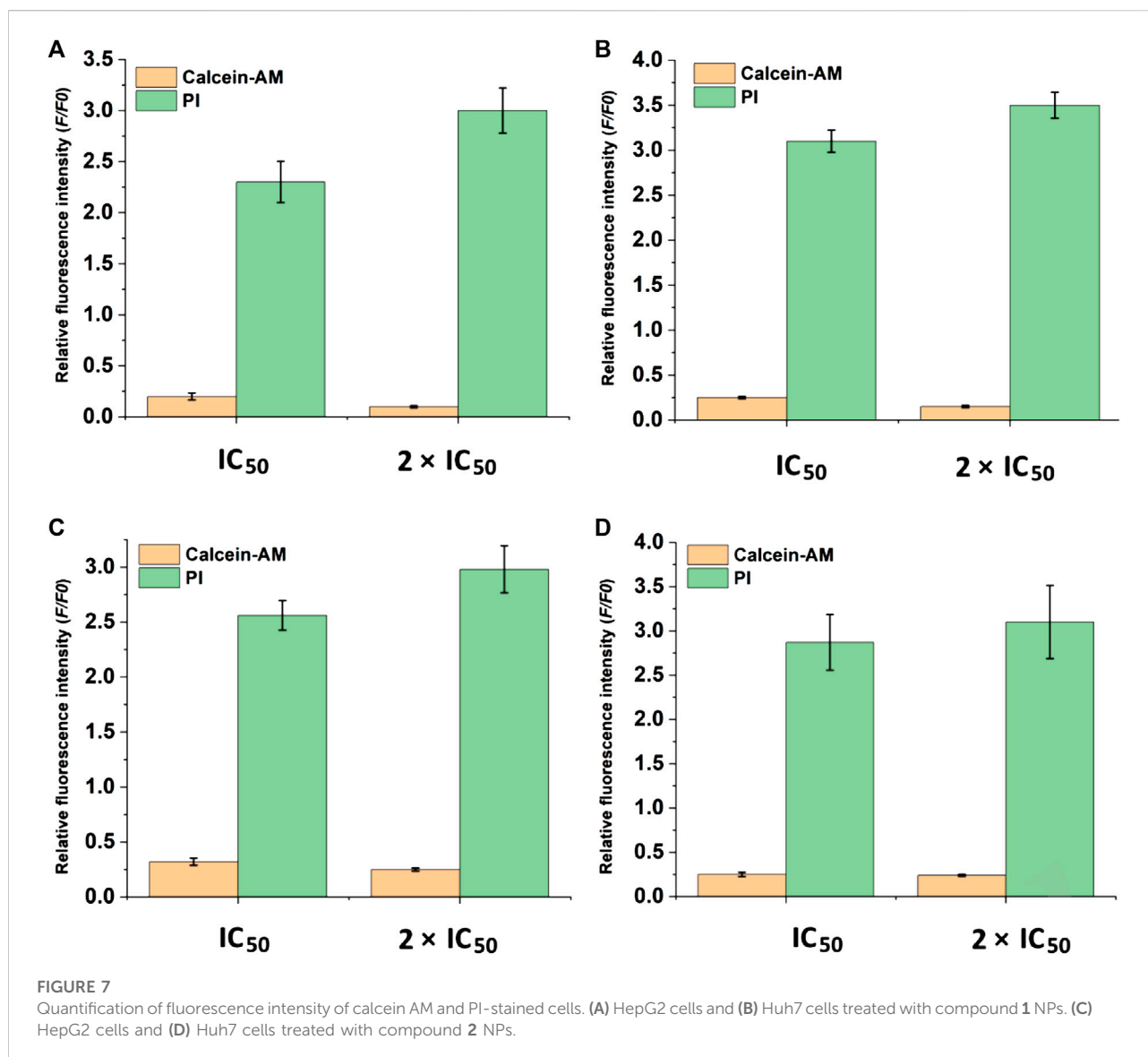
Compound 2 is superior to compound 1 on HepG2 cells, while it is parallel to compound 1 on Huh7 cells in terms of cytotoxicity. Huh7 cells are more sensitive to the NPs containing complexes 1 and 2 than HepG2 cells. Compared with the relevant Cu(II) compounds based on tetrazole ligands, the cytotoxicity of the two compounds is lower than that of [Cu(atzpa)₂] and [Cu(pytzpa)₂] (Zhang et al., 2021) but higher than that of [Cu(2-pytzpa)₂(H₂O)₂].2H₂O (Zhai et al., 2017) (Table 3). The cytotoxicity of these NPs is very low toward healthy hepatocytes because the cell viability remained high (Supplementary Figures S3, S4).

The cytotoxicity of compounds 1 and 2 NPs was further confirmed by flow cytometry, a technique used to detect and measure the physical and chemical characteristics of a population of cells or particles. The results show that the cell apoptotic rates of HepG2 and Huh7 cells in the groups treated with compounds 1 and 2 were significantly increased but markedly different. In particular, all the groups of 2 × IC₅₀ were significantly higher than IC₅₀ groups, and



the apoptosis rates (Q2 + Q3) of the control groups were rather low (Table 4). For the control group, both HepG2 and Huh7 cell viability are very high (87.27% for HepG2 and 93.99% for Huh7), while concentration-dependent cell viability was observed for those treated

with compounds 1 or 2 NPs. These results demonstrated that the compound 1 and compound 2 NPs could induce and promote cell apoptosis of Huh7 and HepG2 cells (Figure 5). Late apoptosis of the cells treated with compound 1 NPs was detected, while both necrosis



and late apoptosis were detected for the cells incubated with compound 2 NPs.

Live/dead co-staining by Calcein-AM and PI

After the discovery of the inhibitory and toxicity effects of compounds 1 and 2 on the HCC cells. The cell viability was investigated by the live/dead co-staining (Figure 6), where living cells can be stained with calcein AM to show green fluorescence and dead cells with PI to exhibit red fluorescence. The cells in control groups expressed large areas of strong green fluorescence, and the faint red fluorescence was almost negligible, indicating that all cells were alive. However, in the groups treated with compound 1 and

compound 2 NPs, a large number of cells were stained with red fluorescence. Cell death is more obvious in the treatment groups with a concentration of 2 × IC₅₀ than that with IC₅₀ (Figure 6). The quantitative fluorescence intensity of the calcein AM and PI also indicates that compounds 1 and 2 NPs can induce cell apoptosis by CDT (Figure 7).

Conclusion

To conclude, two new Cu(II) tetrazole carboxylates were designed and prepared for chemodynamic therapy against HCC. These compounds with new 2D structures are capable of catalyzing H₂O₂ to form cytotoxic hydroxyl radicals, promising their excellent cytotoxicity toward HepG2 and

Huh7 cells. Nanoprecipitation with DSPE-PEG₂₀₀₀ was used to prepare compounds **1** and **2** NPs with good water dispersity. Both the CCK-8 and Calcein-AM/PI co-staining assay confirmed the cytotoxicity of compounds **1** and **2** NPs, which was consistent with the flow cytometry results. Further study is still underway in our group to overcome the H₂O₂ consumption-induced shortage for enhanced chemodynamic therapy, such as H₂O₂ self-supply.

Data availability statement

The data presented in the study are deposited in the <https://pan.baidu.com/s/1pgI7nZDVN1IXKZRmgYcPOA> repository, accession number fic2.

Author contributions

XS, YG, CW, and DZ conceived the study and wrote the manuscript. LS, YZ, and LT synthesized the materials. XS and XJ did the cell experiments. DF re-checked these data.

Acknowledgments

The authors acknowledge financial support from the Scientific Research Pre-Technology Development project of Guilin city (No. 20180104-10), First-class discipline in

References

- Arneth, B. (2020). Tumor microenvironment. *Medicina* 56, 15. doi:10.3390/medicina56010015
- Aromi, G., Barrios, L. A., and Roubeau, O. (2011). Triazoles and tetrazoles: Prime ligands to generate remarkable coordination materials. *Coord. Chem. Rev.* 255, 485–546. doi:10.1016/j.ccr.2010.10.038
- Dai, Y., Shen, T. X., Min, J., Zhang, L. S., Gu, Y. L., and Yang, J. (2021). Synthesis and anticancer property of two Sm(III) compounds based on tetrazole ligands. *Inorganica Chim. Acta* 528, 120598. doi:10.1016/j.ica.2021.120598
- Deng, H. Z., Yang, W. J., Zhou, Z. J., Tian, R., Lin, L. S., Ma, Y., et al. (2020). Targeted scavenging of extracellular ROS relieves suppressive immunogenic cell death. *Nat. Commun.* 11, 4951. doi:10.1038/s41467-020-18745-6
- Du, B. B., Zhu, Y. X., Pan, M., Yue, M. Q., Hou, Y. J., Wu, K., et al. (2015). Direct white-light and a dual-channel barcode module from Pr(III)-MOF crystals. *Chem. Commun.* 51, 12533–12536. doi:10.1039/c5cc04468e
- Fujita, K., Tanaka, Y. Y., Sho, T., Ozeki, S. C., Abe, S., Hikage, T., et al. (2014). Intracellular CO release from composite of ferritin and ruthenium carbonyl complexes. *J. Am. Chem. Soc.* 136, 16902–16908. doi:10.1021/ja508938f
- H Zou, J., Li, L., Zhu, J. W., Li, X. Z., Yang, Z., Huang, W., et al. (2021). Singlet oxygen “afterglow” therapy with NIR-II fluorescent molecules. *Adv. Mat.* 33, 2103627. doi:10.1002/adma.202103627
- Li, L., Zou, J. H., Dai, Y. L., Fan, W. P., Niu, G., Yang, Z., et al. (2020). Burst release of encapsulated annexin A5 in tumours boosts cytotoxic T-cell responses by blocking the phagocytosis of apoptotic cells. *Nat. Biomed. Eng.* 4, 1102–1116. doi:10.1038/s41551-020-0599-5
- Li, X. S., Lee, D. Y., Huang, J. D., and Yoon, J. (2018). Phthalocyanine-assembled nanodots as photosensitizers for highly efficient Type I photoreactions in photodynamic therapy. *Angew. Chem. Int. Ed.* 57, 9885–9890. doi:10.1002/anie.201806551

Guangxi of Traditional Chinese Pharmacology (Direction of Ethnic Medicine) (2018No. 12), and the Autonomous Region Level College Students Innovation and Entrepreneurship Training Program (202010601093 and 202010601164).

Conflict of interest

The authors declare that the research was conducted in the absence of any commercial or financial relationships that could be construed as a potential conflict of interest.

Publisher's note

All claims expressed in this article are solely those of the authors and do not necessarily represent those of their affiliated organizations, or those of the publisher, the editors, and the reviewers. Any product that may be evaluated in this article, or claim that may be made by its manufacturer, is not guaranteed or endorsed by the publisher.

Supplementary material

The Supplementary Material for this article can be found online at: <https://www.frontiersin.org/articles/10.3389/fchem.2022.915247/full#supplementary-material>

- Lin, L. S., Huang, T., Song, J. B., Ou, X. Y., Wang, Z. T., Deng, H. Z., et al. (2019). Synthesis of copper peroxide nanodots for H₂O₂ self-supplying chemodynamic therapy. *J. Am. Chem. Soc.* 141 (25), 9937–9945. doi:10.1021/jacs.9b03457
- Sheldrick, G. M. (2008). A short history of SHELX. *Acta Crystallogr. A* A64, 112–122. doi:10.1107/s0108767307043930
- Shen, J., Chen, J. J., Ke, Z., Zou, D. F., Sun, L. G., and Zou, J. H. (2019). Heavy atom-free semiconducting polymer with high singlet oxygen quantum yield for prostate cancer synergistic phototherapy. *Mat. Chem. Front.* 3, 1123–1127. doi:10.1039/c9qm00158a
- Shen, L., Cao, M. J., Zhang, F. F., Wu, Q., Zhao, L. Y., Lu, Y. M., et al. (2016). Three new manganese(II) coordination complexes based on tetrazole carboxylate ligands. *Transit. Metall. Chem.* 41, 125–131. doi:10.1007/s11243-015-0003-6
- Siegel, R. L., Miller, K. D., and Dvm, A. J. (2018). Cancer statistics, 2018. *Ca. Cancer J. Clin.* 68, 7–30. doi:10.3322/caac.21442
- Song, J. B., Lin, L. S., Yang, Z., Zhu, R., Zhou, Z. J., Li, Z. W., et al. (2019). Self-assembled responsive bilayered vesicles with adjustable oxidative stress for enhanced cancer imaging and therapy. *J. Am. Chem. Soc.* 141, 8158–8170. doi:10.1021/jacs.8b13902
- Sun, F., Yuan, J. W., Li, Y. K., Ju, C. D., Guan, W. H., Yang, G. W., et al. (2016). Substituent-dependent formation of Co(II) complexes based on phenyl-tetrazole acetic acid: From bis- to tristetrazole acetic acid. *Transit. Metall. Chem.* 41, 943–949. doi:10.1007/s11243-016-0099-3
- Sun, W., Li, S. Y., Haupler, B., Liu, J., Jin, S. B., Steffen, W., et al. (2017). Drug therapy: An amphiphilic ruthenium polymetallodrug for combined photodynamic therapy and photochemotherapy *in vivo* (adv. Mater. 6/2017). *Adv. Mat.* 29, 1603. doi:10.1002/adma.201603702
- Sun, W., Thiramanas, R., Slep, L. D., Zeng, X. L., Mail-nder, V., and Wu, S. (2017). *Chem. Eur. J.* 23, 10832–10837. doi:10.1002/chem.201701224

- Tang, W., Yang, Z., Wang, S., Wang, Z., Song, J. B., Yu, G. C., et al. (2018). Organic semiconducting photoacoustic nanodroplets for laser-activatable ultrasound imaging and combinational cancer therapy. *ACS Nano* 12, 2610–2622. doi:10.1021/acsnano.7b08628
- Weiss, A., Berndsen, R., Dubois, M., Müller, C., Schibli, R., Griffioen, A., et al. (2014). *In vivo* anti-tumor activity of the organometallic ruthenium(II)-arene complex [Ru(η^6 -*p*-cymene)Cl₂(pta)] (RAPTA-C) in human ovarian and colorectal carcinomas. *Chem. Sci.* 5, 4742–4748. doi:10.1039/c4sc01255k
- Wriedt, M., Sculley, J. P., Yakovenko, A. A., Ma, Y. G., Halder, G. J., Balbuena, P. B., et al. (2012). Low-Energy selective capture of carbon dioxide by a pre-designed elastic single-molecule trap. *Angew. Chem. Int. Ed.* 51, 9804–9808. doi:10.1002/anie.201202992
- Yang, J., Gu, X. Q., Su, W. T., Hao, X. Y., Shi, Y. J., Zhao, L. Y., et al. (2018). (2-(4-Bromophenyl)ethene-1,1,2-triyl)tribenzene with aggregation induced emission for ablation of HeLa cells. *Mat. Chem. Front.* 2, 1842–1846. doi:10.1039/c8qm00304a
- Yang, J., He, X., Ke, Z., Chen, J. J., Zou, Z. Y., Wei, B., et al. (2020). Two photoactive Ru (II) compounds based on tetrazole ligands for photodynamic therapy. *J. Inorg. Biochem.* 210, 111127. doi:10.1016/j.jinorgbio.2020.111127
- Yang, J., Min, Y. T., Chen, Y., Wang, J., Tian, H., Shen, L., et al. (2014). Syntheses, structures and properties of five coordinating metallic complexes with the new carboxylate-bis(tetrazolyl)amine ligand. *Inorganica Chim. Acta* 419, 73–81. doi:10.1016/j.ica.2014.04.013
- Yang, J., Xu, Y., Jiang, M., Zou, D. F., Yang, G. W., Shen, L., et al. (2019). Photochemical property of two Ru(II) compounds based on 5-(2-pyrazinyl) tetrazole for cancer phototherapy by changing auxiliary ligand. *J. Inorg. Biochem.* 193, 124–129. doi:10.1016/j.jinorgbio.2019.01.015
- Yang, Z., Fan, W. P., Zou, J. H., Tang, W., Li, L., He, L. C., et al. (2019). Precision cancer theranostic platform by *in situ* polymerization in perylene diimide-hybridized hollow mesoporous organosilica nanoparticles. *J. Am. Chem. Soc.* 141, 14687–14698. doi:10.1021/jacs.9b06086
- Yang, Z., Song, J. B., Tang, W., Fan, W. P., Dai, Y. L., Shen, Z. Y., et al. (2019). Stimuli-responsive nanotheranostics for real-time monitoring drug release by photoacoustic imaging. *Theranostics* 9, 526–536. doi:10.7150/thno.30779
- Zhai, C., Zhao, L., Hao, X. Y., Shi, Y. J., Xu, D., Yang, Z. Y., et al. (2017). One Cu(II) compound derived from 5-(2-pyridyl)tetrazole-2-isopropanoic acid against HeLa cells. *Inorg. Chem. Commun.* 84, 150–152. doi:10.1016/j.inoche.2017.08.018
- Zhang, A. L., Li, X. C., Min, J., Tan, L. T., Xu, H. L., Zhu, X. G., et al. (2021). Synthesis and anticancer property of three new Cu(II) coordination polymers constructed by the bifunctional substituted-poly nitrogen heterocyclic ligands. *Inorganica Chim. Acta* 522, 120380. doi:10.1016/j.ica.2021.120380
- Zhang, S., Yang, Q., Liu, X. Y., Qu, X. N., Wei, Q., Xie, G., et al. (2016). High-energy metal-organic frameworks (HE-MOFs): Synthesis, structure and energetic performance. *Coord. Chem. Rev.* 307, 292–312. doi:10.1016/j.ccr.2015.08.006
- Zhu, H. T. C., Li, Q., Shi, B. B., Ge, F. J., Liu, Y. Z., Mao, Z. W., et al. (2020). Dual-emissive platinum(II) metallacage with a sensitive oxygen response for imaging of hypoxia and imaging-guided chemotherapy. *Angew. Chem. Int. Ed.* 59, 20208–20214. doi:10.1002/anie.202009442
- Zou, J. H., Chen, D. Y., Yang, G. W., Li, Q. Y., Yang, J., and Shen, L. (2015). Synthesis, crystal structure and catalytic property of a new samarium compound derived from 5-(pyrazin-2-yl)tetrazole-2-acetic acid. *RSC Adv.* 5, 27887–27890. doi:10.1039/c5ra03296b
- Zou, J. H., Cui, H. J., Xu, B., Zhu, D. L., Li, Q. Y., Yang, G. W., et al. (2014). Three new alkaline Earth coordination compounds based on 5-(2-pyrimidyl)tetrazole-2-acetic acid. *Inorganica Chim. Acta* 423, 430–434. doi:10.1016/j.ica.2014.08.058
- Zou, J. H., Li, L., Yang, Z., and Chen, X. Y. (2021). Phototherapy meets immunotherapy: A win-win strategy to fight against cancer. *Nanophotonics* 10, 3229–3245. doi:10.1515/nanoph-2021-0209
- Zou, J. H., Wu, H., Zhu, D. L., Tian, H., Zhang, P., Zhao, L. Y., et al. (2014). pH-dependent synthesis of a cadmium coordination compound from a compound based on Hpytz ligand [Hpytz = 5-(4-pyridyl)tetrazole]. *J. Coord. Chem.* 67, 3444–3453. doi:10.1080/00958972.2014.965163
- Zou, J. H., Zhu, D. L., Li, F. F., Li, F. S., Wu, H., Li, Q. Y., et al. (2014). Three new coordination compounds with neodymium based on tetrazole containing carboxylic acid ligands. *Z. Anorg. Allg. Chem.* 640, 2226–2231. doi:10.1002/zaac.201400106
- Zou, J. H., Zhu, D. L., Liu, Q., Li, S., Mei, G. D., Zhu, J. N., et al. (2014). Four new zinc coordination compounds derived from various tetrazole-containing carboxylic acids and 4,4'-bipyridine. *Inorganica Chim. Acta* 421, 451–458. doi:10.1016/j.ica.2014.06.029
- Zou, J. H., Zhu, D. L., Tian, H., Li, F. F., Zhang, F. F., Yang, G. W., et al. (2014). Construction of six new coordination complexes with 5-(3-pyridyl) tetrazole-2-acetate. *Inorganica Chim. Acta* 423, 87–94. doi:10.1016/j.ica.2014.07.034
- Zou, J. H., Zhu, J. N., Cui, H. J., Wang, Z., Zhu, D. L., Zhang, F. F., et al. (2015). Group position-dependent structurally diverse coordination compounds based on isomeric ligands. *Aust. J. Chem.* 68, 889. doi:10.1071/ch14442
- Zou, J. H., Zhu, J. W., Yang, Z., Li, L., Fan, W. P., He, L. C., et al. (2020). A phototheranostic strategy to continuously deliver singlet oxygen in the dark and hypoxic tumor microenvironment. *Angew. Chem. Int. Ed.* 59, 8833–8838. doi:10.1002/anie.201914384